J. Braz. Chem. Soc., Vol. 15, No. 4, 541-547, 2004.
Printed in Brazil - ©2004 Sociedade Brasileira de Química
0103 - 5053 $6.00+0.00

Article

Behavior of a Co-Cr-Mo Biomaterial in Simulated Body Fluid Solutions Studied by Electrochemical and Surface Analysis Techniques

Fernando Carlos Giacomelli, Cristiano Giacomelli and Almir Spinelli*

Departamento de Química, Universidade Federal de Santa Catarina, 88040-900 Florianópolis - SC, Brazil

O comportamento do biomaterial Co-Cr-Mo (usado em próteses dentárias) em saliva artificial (AFNOR S90-701), saliva artificial com temperatura e pH modificados e contendo fluoreto foi estudado por técnicas eletroquímicas (potencial de circuito aberto e polarização potenciodinâmica) e de análise de superfície (Microscopia Eletrônica de Varredura (MEV) e Espectroscopia de Energia Dispersiva (EED)). Os resultados revelaram que a morfologia da superfície após a polarização potenciodinâmica é heterogênea, exibindo três regiões de composição distinta. Espécies solúveis como CrO_4^{2-} foram liberadas para a solução durante a polarização. A temperatura e o pH da solução exerceram influência acentuada sobre a cinética de dissolução do biomaterial, enquanto que a presença de fluoreto não alterou as características do sistema.

The behavior of a Co-Cr-Mo biomaterial used as dental prosthesis was studied by electrochemical (Open Circuit Potential (OCP) and potentiodynamic polarization) and surface analysis techniques (Scanning Electron Microscopy (SEM) and Energy Dispersive Spectroscopy (EDS)) in artificial saliva, artificial saliva with modified temperature (7 ºC – 47 ºC) and pH (1.4 – 13.4), and containing fluoride (1500 ppm). The results revealed that the surface morphology after potentiodynamic polarization is highly heterogeneous exhibiting three regions of different composition. Soluble metal species such as CrO_4^{2-} were released to the solution during the potentiodynamic polarization. The electrochemical processes were markedly influenced by solution temperature and pH, whereas the presence of fluoride did not produce changes in the system.

Keywords*:* biomaterial, Co-Cr-Mo alloy, electrochemical behavior, surface analysis

Introduction

The employment of metal prostheses in substitution to damaged members of the human body has been reported since a long time ago, and they were widely applied during the Second World War. However, catastrophic results occurred basically due to the use of non-biocompatible metals in their fabrication. Consequently, the scientific community has been involved in a crescent effort not only to develop new metal alloys but also to understand their interaction with the human body in terms of corrosion behavior, mechanical properties, biocompatibility and biofunctionality.[1] Co-Cr-Mo alloys have already been used as cutting tools, valves of safety, turbines and strategic materials since the beginning of the 20th century.[2] Currently, they are also employed in bolts, screws and, in particular, in orthodontic prostheses.[3-5] These alloys present good corrosion resistance[6] and excellent mechanical properties, especially when nitrogen is added.[3,7]

When metal alloys are used as implants, a comprehensive knowledge of their effect on the surrounding tissues is required. For example, the oxidation of Co-Cr-Mo may produce soluble Co and Cr species, which can be released to the neighboring tissues. Depending on the nature and concentration of such chemical species, several adverse reactions may take place, including cytotoxicity,[8-10] allergic[11-13] and carcinogenic effects,[13] irritant reactions[14] and local symptoms in gingiva when used as dental implants.[15] Therefore, Co-Cr-Mo alloys still request for an insight into their electrochemical behavior and corrosion resistance not only in artificial saliva but also in most unfavorable environment such as aggressive pH.

We report here on the electrochemical behavior and corrosion resistance *in vitro* of a Co-Cr-Mo alloy in artificial saliva (AFNOR S90-701) and in artificial saliva with modified pH and temperature, and in presence of fluoride. The surface condition after corrosion

* e-mail: spin@qmc.ufsc.br

measurements was evaluated by Scanning Electron Microscopy (SEM) and Energy Dispersive Spectroscopy (EDS) techniques.

Experimental

Materials

A Co-Cr-Mo alloy with composition very close to that of ASTM F75 alloy was employed. Artificial saliva AFNOR S90-701 was used as working solution and prepared using reagents of analytical grade without previous purification. When it was necessary, the pH was adjusted by adding H_3PO_4 or NaOH diluted solutions. Both the Co-Cr-Mo alloy and the AFNOR S90-701 artificial saliva compositions are given in Table 1.

Table 1. Chemical composition of the Co-Cr-Mo alloy and AFNOR S90-701 artificial saliva

Co-Cr-Mo alloy composition[a]				
	Co	Cr	Mo	Ni and Fe
% wt	65	28	5	Balance
AFNOR S90-701 Artificial Saliva composition / g L^{-1}				
Na_2HPO_4	0.26			
NaCl	6.70			
KSCN	0.33			
KH_2PO_4	0.20			
KCl	1.20			
$NaHCO_3$	1.50			

[a] Determined by atomic absorption spectroscopy.

Electrochemical system

Electrochemical measurements were carried out with an EG&G PAR model 263A potentiostat/galvanostat interfaced to a personal computer using the EG&G-PAR "SoftCorr II Model 252/352" software for data acquisition and analysis. The electrochemical cell contained five openings: three of them were used for the electrodes and two of them for nitrogen bubbling prior to all the experiments or to keep an inert atmosphere by a flow through the cell also during all the experiments. The counter electrode (CE) was a graphite rod and the reference electrode (RE) was a saturated calomel electrode (SCE) connected to the cell by a salt bridge and a Luggin-Habber capillary. All potentials in the text are quoted to this electrode. The working electrode (WE) was a 0.55 cm^2 (geometrical surface area) Co-Cr-Mo disc mounted in a glass tube with Araldite® epoxy. Prior to the experiments, the electrode surface was polished with 1200 emery paper, ultrasonically cleaned, degreased with acetone, rinsed with deionized water, and finally air-dried. The potentiodynamic polarization curves were recorded in agreement with the ASTM G5 norm. Electrochemical experiments were performed after an electro-reduction process at a fixed potential ($E_{\lambda,c}$ = -1.12 V/SCE) in order to reduce as much as possible the spontaneously formed oxides onto the electrode surface and improve reproducibility. Excellent reproducibility was achieved when a potentiostatic reduction during 10 min was applied. The corrosion current density (j_{corr}) was determined by extrapolation to E(I=0) (the potential where the current density is zero) of the anodic and cathodic curve branch in the potentiodynamic polarization curves.

Surface analysis

Surface morphology was observed by Scanning Electron Microscopy (SEM) before and after the electrochemical experiments using a Philips XL-30 microscope. In both cases, the specimens were exposed to the atmosphere. Surface composition was determined by an Energy Dispersive Spectroscopy (EDS) apparatus coupled to the Philips XL-30 microscope.

Results and Discussion

Figure 1 shows the open circuit potential (OCP) (A) and potentiodynamic polarization (B) curves for a Co-Cr-Mo stationary electrode immersed in AFNOR S90-701 artificial saliva at 37 ºC and pH 7.4. Following the immersion, an abrupt OCP displacement towards positive potentials was noticed in Figure 1A during a period of 10-15 min. Afterwards, the OCP remained slowly increasing, suggesting the growth of a film onto the metallic surface. After 60 min exposure, an approximately constant value of -790 ± 17 mV was attained, and this value was taken as the corrosion potential (E_{corr}). The potentiodynamic polarization curves given in Figure 1B showed the alloy directly translated to a stable passive behavior from the Tafel region without exhibiting an active-passive transition. The electrode passivity was observed for a large potential range (approximately 1.0 V) from -750 mV to +310 mV. At more positive potentials, the current density increased due to both transpassivation and oxygen evolution reaction. Furthermore, three oxidation peaks were observed, as indicated in Figure 1B. Peak I (-460 mV) was attributed to the electrochemical oxidation of cobalt in agreement with Silva *et al.*[16] Peak II (+520 mV) and peak III (+760 mV) were ascribed to electrochemical reactions involving transitions to high oxidation states of chromium.[17] Pan *et al.*[18] recorded a small current peak at +650 mV/SCE in chromium-nickel based alloys, which was attributed to the electrochemical oxidation of

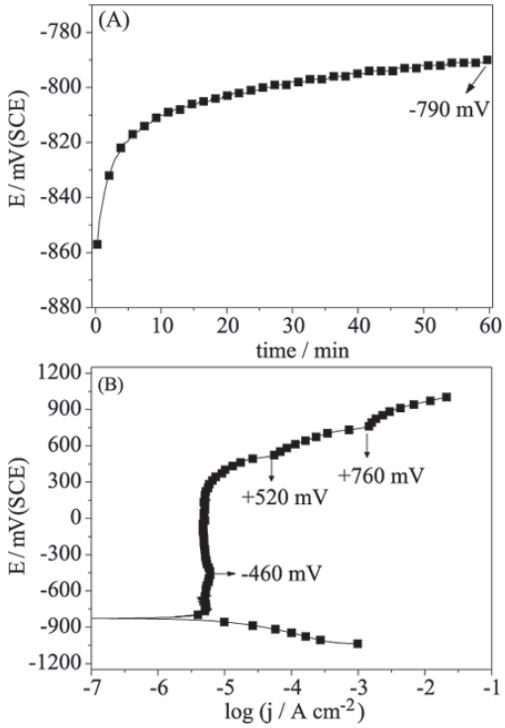

Figure 1. OCP (A) and potentiodynamic polarization (B) curves for a Co-Cr-Mo stationary electrode immersed in AFNOR S90-701 artificial saliva at 37 ºC and pH 7.4.

chromium. The corrosion current density (j_{corr}) extracted from the potentiodynamic polarization curve in Figure 1B was 6.8 ± 1.0 μA cm^{-2}.

Figure 2 shows SEM micrographs for untreated Co-Cr-Mo alloy (before electrochemical experiment - Figure 2A) and after potentiodynamic polarization (Figure 2B). In Figure 2A the surface is homogenous presenting some porous from the substrate. Upon potentiodynamic polarization (from –0.25 V/E_{corr} to +1.2 V/SCE)), the surface became completely heterogeneous showing at least three distinct regions (**a**, **b** and **c**), as indicated. In order to better understand this behavior, EDS semi quantitative microanalysis was performed on untreated samples and after the potentiodynamic polarization tests in several experimental conditions. The results are given in Table 2, where only the alloy elements are shown, and the results correspond to analyses of the overall surface, *i.e.*, the distinct regions were not taken into consideration. The Co content decreased from 56.54% for untreated samples to 39.04% after polarization at 37 ºC and pH 7.4. On the other hand, Mo and Cr contents did not show pronounced changes. When local analysis was done at each region depicted in Figure 2B, different composition was observed for **a**, **b** and **c** (Table 3). **a** and **b** are regions enriched with Mo and Cr (**a**) and Co (**b**) when compared with the surface composition of untreated samples (Table 2).

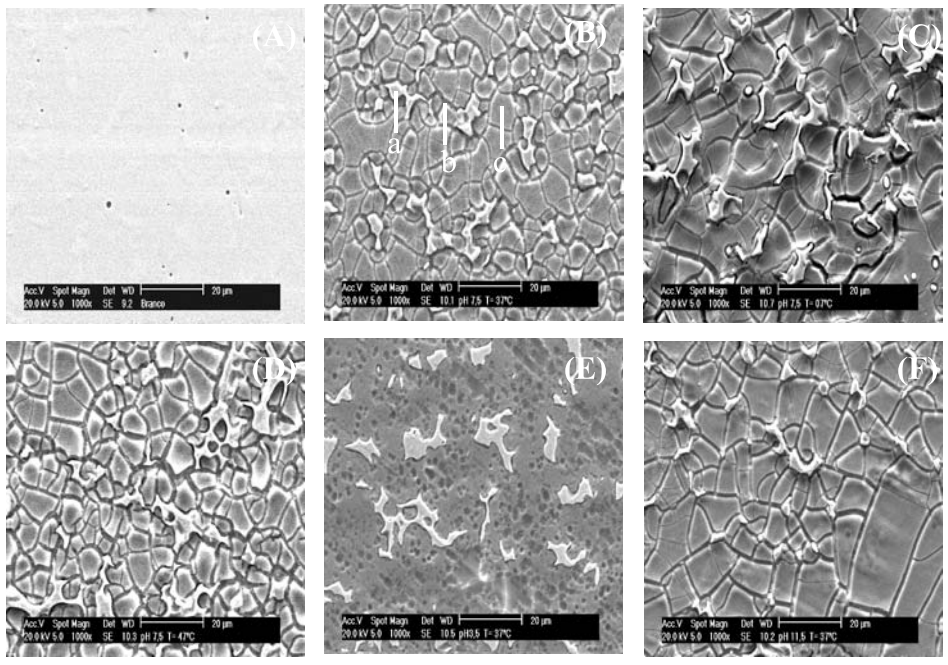

Figure 2. SEM micrographs of a Co-Cr-Mo alloy surface before any electrochemical measurement (A) and after potentiodynamic polarization tests in different pH/temperature conditions: 7.4/37 ºC (B), 7.4/7 ºC (C), 7.4/47 ºC (D), 3.4/37 ºC (E) and 11.4/37 ºC (F).

Table 2. Semi quantitative data from EDS surface analyses obtained for an untreated sample and after potentiodynamic polarization tests in different experimental conditions (the values are given in % wt)

pH	3.4	7.4			11.4	untreated
T / ºC	37	7	37[a]	47	37	sample[b]
Co	41.59	43.68	39.04	35.12	46.07	56.54
Cr	21.27	20.62	20.99	20.50	18.38	22.33
Mo	6.95	5.16	5.45	5.04	4.96	5.19

[a] AFNOR S90-701 artificial saliva; [b] EDS results obtained before electrochemical experiments.

Table 3. Semi quantitative data from EDS local analyses at regions **a**, **b** and **c** indicated in Figure 2B[a] (values are given in % wt)

	region		
Mo	15.07	4.16	3.18

[a] after potentiodynamic polarization in AFNOR S90-701 artificial saliva.

Although potential limit (+1.2 V/SCE) to which the electrode was submitted may not stand for physiological conditions, the authors consider these results really important since Co-Cr-Mo was shown to dissolve heterogeneously, with possible implications in biocompatibility. It is known that pure Ti in the human body may be exposed to potentials of up to 450-550 mV/SCE.[19] Unfortunately, the same information was not found for Co-Cr-Mo biomaterial. However, the potential-pH diagram given by Black[20] for physiological conditions generically showed that the potential value of a metallic biomaterial may vary from -1.0 to 1.2 V in the human body.

Effect of temperature

Figure 3 shows the E_{corr} extracted from OCP curves (A) and the potentiodynamic polarization curves (B) for Co-Cr-Mo stationary electrodes immersed in AFNOR S90-701 artificial saliva (pH 7.4) at different temperatures ranging form 7 ºC to 47 ºC. The E_{corr} in Figure 3A was practically not affected by temperature, suggesting that almost identical compositions at the interface film/solution as function of temperature evolved during immersion, since a variation in E_{corr} is only possible when there are changes in the composition parameter at this interface.[21] The potentiodynamic polarization curves in Figure 3B did not show important profile changes. However, j_{corr} was found to be dependent on the temperature. The corrosion current density, j_{corr}, was extracted from Figure 3B and plotted against the temperature (Figure 4). The j_{corr} determined at 47 ºC (9.0 ± 1.4 μA cm^{-2}) was about 5 times higher than at 7 ºC (2.0 ±

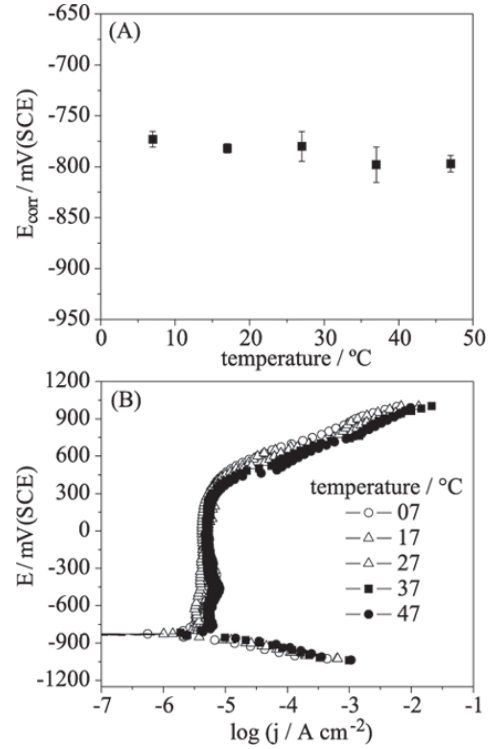

Figure 3. OCP-values measured after 60 min of immersion (E_{corr}-values) (A) and potentiodynamic polarization curves (B) for a Co-Cr-Mo stationary electrode immersed in AFNOR S90-701 artificial saliva with pH 7.4 and different temperatures.

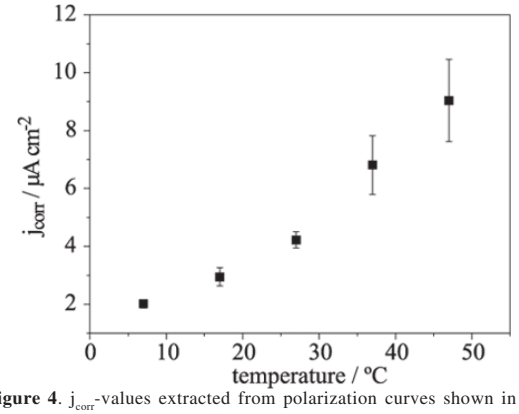

Figure 4. j_{corr}-values extracted from polarization curves shown in Figure 3B against the temperature.

0.1 μA cm^{-2}), indicating that the dissolution increased with the temperature. The surface morphology after potentiodynamic polarization in solutions thermostated at different temperatures presented almost the same characteristics as those already described, as shown in Figures 2B, 2C and 2D for 37, 7 and 47 ºC, respectively. However, the Co content after potentiodynamic polarization varied (Table 2). Increasing temperature, the cobalt concentration decreased (43.68 % at 7 ºC to 35.12 % at 47 ºC). It is important to note that the results from EDS analyses suggesting variable surface compositions as function of temperature do not contradict the findings above described on basis of Figure 3A. In that case, the Co-Cr-Mo electrodes were not submitted to polarization.

Effect of pH

The influence of pH on the E_{corr} of Co-Cr-Mo stationary electrodes immersed in AFNOR S90-701 artificial saliva with modified pH at 37 ºC is shown in Figure 5. E_{corr} was a function of pH over the entire range (1.4 – 13.4), generating a straight line with $\delta E_{corr}\ \delta pH^{-1}$ = -55 mV pH^{-1} (a value close to that of pH indicator electrodes,[22] in particular for Mo electrodes in aqueous media, which have been used as pH sensors at high temperatures).[23] This behavior also suggested that distinct composition at the interface electrode/solution evolved during immersion as function of pH.

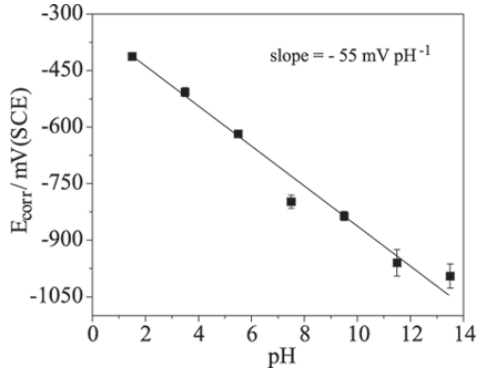

Figure 5. OCP measured after 60 min of immersion (E_{corr}-value) in AFNOR S90-701 artificial saliva and artificial saliva with modified pH for a Co-Cr-Mo stationary electrode at 37 ºC.

Figure 6 shows the potentiodynamic polarization curves recorded for Co-Cr-Mo stationary electrodes immersed in solutions with different pH at 37 ºC. The curve at pH 7.4 was included in both figures as reference. It was observed that peak I is pronounced in solutions with pH < 7.4, while its intensity decreased at pH > 7.4. This process was pH-dependent with $\delta E^{I}\delta pH^{-1}$ = -96 mV pH^{-1} for pH Ω7.4, and

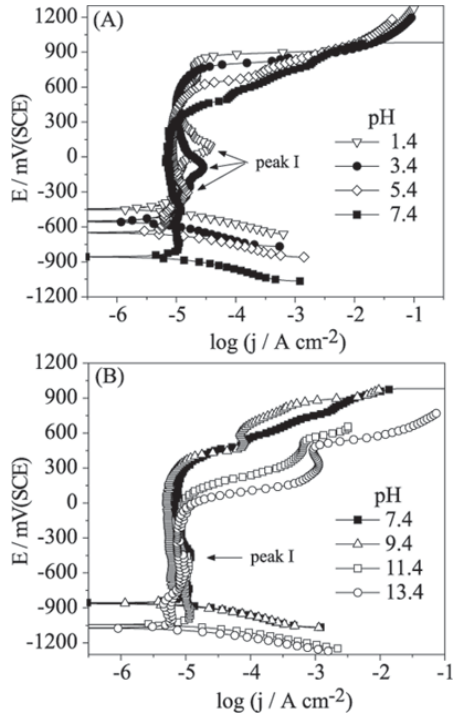

Figure 6. Potentiodynamic polarization curves monitored in acid (A) and basic (B) solutions at 37 ºC for a Co-Cr-Mo stationary electrode.

was associated to the oxidation involving Co species in the passive oxide layer. For solutions with pH > 7.4 (Figure 6B), the oxidation of chromium (at *ca*. +0.30 V at pH 13.4) became gradually more evident as the pH increased.

Figure 7 shows the variation of j_{corr} (extracted from the potentiodynamic polarization curves shown in Figure 6B) as a function of pH. In the range of 3.4 < pH < 11.4, j_{corr} was a linear function of pH, the maximum j_{corr} found in pH 11.4 (j_{corr} = 12.3 ± 1.2 μA cm^{-2}) and minimum in pH 3.4 (j_{corr} = 4.2 ± 0.1 μA cm^{-2}).

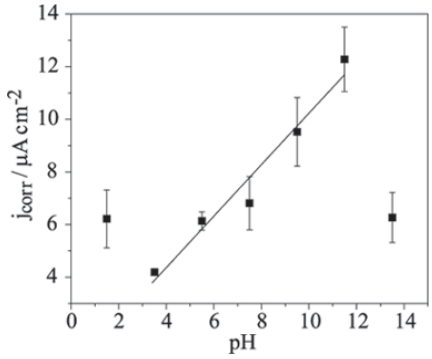

Figure 7. j_{corr}-values extracted from polarization curves shown in Figure 6 against pH.

A SEM micrograph recorded for a Co-Cr-Mo electrode after potentiodynamic polarization at pH 3.4 is shown in Figure 2E. The morphology was entirely different from those obtained for electrodes immersed at pH 7.4 (Figure 2B) and 11.4 (Figure 2F). From the EDS results in Table 2, the higher cobalt content on the surface was observed for electrodes immersed in pH 11.4 solutions. At pH 3.4, an increase in molybdenum content was noticed when compared with the results obtained in artificial saliva at pH 7.4.

In the range of 3.4 < pH < 11.4 the dissolution increased as a function of pH (Figure 7) due to the formation of soluble species of Co, Cr and Mo. During the potentiodynamic polarization at high potentials (above +0.50 V) the working solution became yellow when the pH was higher than 7.4, and its qualitative analysis revealed the presence of Co, Cr and Mo. The opposite behavior was, however, observed in acid solutions where stable molybdenum oxides (MoO_3 and MoO_2) can be formed. These facts were in agreement with the findings from EDS microanalysis and with the thermodynamic stability of Co, Cr and Mo in aqueous solutions represented by Pourbaix diagrams.[24]

Regarding the heterogeneous morphology verified through SEM analyses (Figure 2), it is believed that the dissolution process comes initially from a number of active centers, and since the molybdenum has a high importance in reduction of alloy dissolution even in small quantities, it might be acting in these centers originating the heterogeneous surfaces in Figures 2B-F. This statement was firstly proposed by Kolotyrkin[25,26] in his studies on the dissolution of Fe-Cr alloys containing small quantities of Mo in sulfuric acid solutions. Also, it is important to observe that the working solution was a complex mixture of salts. The role of anions in active dissolution processes of metals in aqueous solutions consists in their influence on the composition of the surface species, thereby establishing competitive adsorption of different species and originating active centers.[26,27]

Effect of fluoride

Fluoride ions present negative influence on the electrochemical behavior of some metallic biomaterials, specially Ti-based alloys due to the complexing reaction between Ti and F^- yielding TiF_6^{2-}, a species with high constant of formation,[28] originating localized corrosion.[29-31]

In order to verify the possible influence also on the Co-Cr-Mo behavior, experiments were performed in presence of fluoride in artificial saliva and in artificial saliva with pH 5.4. Figure 8 shows OCP (A) and the potentiodynamic polarization curves (B) recorded in AFNOR S90-701 artificial saliva and in artificial saliva with pH 5.4 for Co-Cr-Mo stationary electrodes in presence and in absence of 1500 ppm fluoride (the typical concentration in commercial fluoridated toothpastes and mouthwash). No changes were observed comparing the curves monitored in presence and absence of fluoride. The same comment can also be extended to the surface morphology and j_{corr}.

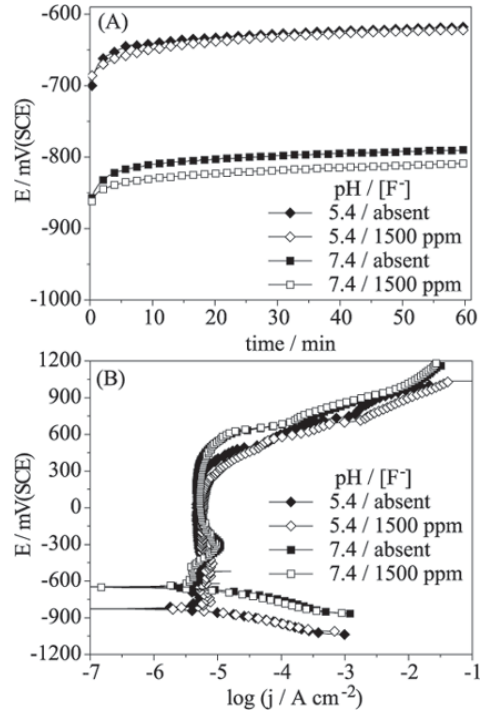

Figure 8. OCP (A) and potentiodynamic polarization curves (B) monitored in AFNOR S90-701 artificial saliva and in artificial saliva with pH 5.4 for a Co-Cr-Mo stationary electrode in presence and absence of fluoride.

Conclusion

The results obtained in this work by employing electrochemical, microscopic and spectroscopic techniques showed the electrochemical and corrosion behavior of a Co-Cr-Mo alloy in artificial saliva (AFNOR S90-701), artificial saliva with modified temperature (7 ºC – 47 ºC) and pH (1.4 – 13.4), and containing fluoride (1500 ppm). The influence of each variable was investigated by analyzing E_{corr} and j_{corr} values and the composition and morphology of the electrode surface. The E_{corr} was not influenced by the temperature or fluoride ions, however it was a linear function of pH. Similarly, j_{corr} depended on the temperature and pH. The effect of

temperature was assigned to the increase in the solubility product of species formed on the electrode surface, provoking a simultaneous j_{corr} increase. The influence of pH was explained on basis of the thermodynamic stability of soluble and solid species formed from each alloy constituent. SEM micrographs revealed that the surface morphology after potentiodynamic polarization is highly heterogeneous, exhibiting three regions of different composition. The addition of 1500 ppm fluoride ions did not promote appreciable changes.

Acknowledgements

The authors are grateful to CNPq – Conselho Nacional de Desenvolvimento Científico e Tecnológico – for financial support. C. Giacomelli whishes to thank to CAPES – Coordenação de Aperfeiçoamento de Pessoal de Nível Superior.

References

1. Lemons, J.; Venugopalan, R.; Lucas, L. In *Corrosion and Biodegradation*; A. Von Recum, ed., Taylor Francis Inc: New York, 1999, p. 155.
2. Codaro, E. N.; Melnikov, P.; Ramires, I.; Guastaldi, A. C.; *Russ. J. Electrochem.* **2000**, *36*, 1117.
3. Escobedo, J.; Mendez, J.; Cortes, D.; Gomez, J.; Mendez, M.; Mancha, H.; *Mater. Des.* **1996**, *17*, 79.
4. Hsu, H. C.; Yen, S. K.; *Dent. Mater.* **1998**, *14*, 339.
5. Yen, S. K.; Guo, M. J.; Zan, H. Z.; *Biomaterials* **2001**, *22*, 125.
6. He, D.; Zhang, T.; Wu, Y.; *Wear* **2001**, *250*, 180.
7. Kilner, T.; Dempsey, A. J.; Pilliar, R. M.; Weatherly, G. C.; *J. Mater. Sci.* **1987**, *22*, 565.
8. Stenberg, T.; *Scand. J. Dent. Res.* **1982**, *90*, 472.
9. Messer, R. L. W.; Lucas, L. C.; *Dent. Mater.* **2000**, *16*, 207.
10. Ermolli, M.; Menne, C.; Pozzi, G.; Serra, M. A.; Clerici, L. A.; *Toxicology* **2001**, *159*, 23.
11. van Joost, T.; van Everdingen, J. J.; *Acta. Derm. Venereol.* **1982**, *62*, 525.
12. Vestey, J. P.; Gawkrodger, D. J.; Wong, W. K.; Buxton, P. K.; *Contact Dermatitis* **1986**, *15*, 119.
13. Bouchard, P. R.; Black, J.; Albrecht, B. A.; Kaderly, R. E.; Galante, J. O.; Pauli, B. U.; *J. Biomed. Mater. Res.* **1996**, *32*, 37.
14. Rystedt, I.; Fisher, T.; *Contact Dermatitis* **1985**, *12*, 93.
15. Arvidson, K.; Cottlerfox, M.; Friberg, U.; *J. Dent. Res.* **1980**, *59*, 651.
16. Silva, A. Y. V.; Baldissera, S.; Amaral, J. C.; Codaro, E. N.; Nakazato, R. Z.; Felipe, H.; *XIII Simpósio Brasileiro de Eletroquímica e Eletroanalítica*, Araraquara, Brazil, 2002.
17. Valéria, A. A.; Christopher, M. A. B.; *Corr. Sci.* **2002**, *44*, 1949.
18. Pan, J.; Karlen, C.; Ulfvin, C.; *J. Electrochem. Soc.* **2000**, *147*, 1021.
19. Rondelli, G.; Vicentini, B.; *Biomaterials* **2002**, *23*, 639.
20. Black, J. In *Biological Performance of Materials: Fundamentals of Biocompatibility*; Marcel Decker Inc.: New York, 1992.
21. Vetter, K. J.; *Electrochim. Acta* **1971**, *16*, 1923.
22. AlKharafi, F. M.; Badawy, W. A.; *Electrochim. Acta* **1997**, *42*, 579.
23. Badawy, W. A.; Al-Kharafi, F. M.; *Electrochim. Acta* **1998**, *44*, 693.
24. Pourbaix, M.; *Atlas of Electrochemical Equilibria in Aqueous Solutions*, Pergamon Press: London, 1996.
25. Kolotyrkin, Y. M.; Plaskeev, A. V.; Knyazheva, V. M.; Kozhevnikov, V. B.; Raskin, G. S.; *Dokl Akad Nauk SSSR* **1978**, *243*, 1483.
26. Kolotyrkin, Y. M.; *Electrochim. Acta* **1980**, *25*, 89.
27. Florianovich, G. M.; Lazorenko-Manevich, R. M.; *Electrochim. Acta* **1997,** *42*, 879.
28. Fovet, Y.; Gal, J. Y.; Toumelin-Chemla, F.; *Talanta* **2001**, *53*, 1053.
29. Huang, H.-H.; *Biomaterials* **2003**, *24*, 275.
30. Rondelli, G.; Vicentini, B.; *Biomaterials* **1999**, *20*, 785.
31. Schiff, N.; Grosgogeat, B.; Lissac, M.; Dalard, F.; *Biomaterials* **2002**, *23*, 1995.

Received: November 10, 2003
Published on the web: July 8, 2004